The Deeper the Better? A Thermogeological Analysis of Medium-deep Borehole Heat Exchanger Efficiency in Crystalline Rocks

Kaiu Piipponen (kaiu.piipponen@gtk.fi)
Geological Survey of Finland: Geologian tutkimuskeskus https://orcid.org/0000-0002-2969-7521
Annu Martinkauppi
Geological Survey of Finland: Geologian tutkimuskeskus
Sami Vallin
Geological Survey of Finland: Geologian tutkimuskeskus
Teppo Arola
Geological Survey of Finland, Geologian tutkimuskeskus
Nina Leppäharju
Geological Survey of Finland, Geologian tutkimuskeskus
Kimmo Korhonen
Geological Survey of Finland, Geologian tutkimuskeskus
Alan Bischoff
Geological Survey of Finland, Geologian tutkimuskeskus

Research

Keywords: Geothermal energy, medium-deep, low enthalpy, borehole heat exchanger, crystalline rock, COMSOL Multiphysics, space heating

Posted Date: January 5th, 2022

DOI: https://doi.org/10.21203/rs.3.rs-1196300/v1

The deeper the better? A thermogeological analysis of medium-deep borehole heat exchanger efficiency in crystalline rocks

Authors:

Kaiu Piipponen[1*], Annu Martinkauppi[2], Sami Vallin[1], Teppo Arola[1], Nina Leppäharju[1], Kimmo Korhonen[1], Alan Bischoff[1]

* Corresponding author, kaiu.piipponen@gtk.fi

[1] Geological Survey of Finland, Vuorimiehentie 5, PL 96, 02151 Espoo, Finland

[2] Geological Survey of Finland, Teknologiankatu 7, PL 97, 67101 Kokkola, Finland

Abstract

The energy sector is undergoing a fundamental transformation, with significant investment in low-carbon technologies to replace fossil-based systems. In densely populated urban areas, deep boreholes offer an alternative over shallow geothermal systems, which demand extensive surface area to attain large-scale heat production. This paper presents numerical calculations of the thermal energy that can be extracted from the medium-deep borehole heat exchangers of depths ranging from 600-3000 m. We applied the thermogeological parameters of three locations across Finland and tested two types of coaxial borehole heat exchangers to understand better the variables that affect heat production in low permeability crystalline rocks. For each depth, location, and heat collector type, we used a range of fluid flow rates to examine the correlation between thermal energy production and resulting outlet temperature. Our results indicate a trade-off between thermal energy production and outlet fluid temperature depending on the fluid flow rate, and that the vacuum-insulated tubing outperforms high-density polyethylene pipe in energy and temperature production. In addition, the results suggest that the local thermogeological factors impact heat production. Maximum energy production from a 600-m-deep well achieved 170 MWh/a, increasing to 330 MWh/a from a 1000-m-deep well, 980 MWh/a from a 2-km-deep well, and up to 1880 MWh/a from a 3-km-deep well. We demonstrate that understanding the interplay of the local geology, heat exchanger materials, and fluid circulation rates is necessary to maximize the potential of medium-deep geothermal boreholes as a reliable long-term baseload energy source.

Keywords: Geothermal energy, medium-deep, low enthalpy, borehole heat exchanger, crystalline rock, COMSOL Multiphysics, space heating

Introduction

The progressive displacement of fossil fuels by clean, affordable, and reliable energy sources requires implementation of low-carbon technologies that will meet large-scale commercial demands across all energy sectors. Low-carbon renewable heat production at large scales is a challenging target for most cold climate countries, today accounting for only a minor proportion of the energy used for space heating worldwide (IEA, 2021). Whereas countries like Finland and Denmark can provide over 50% of their space heating needs from renewables, petroleum-based sources are still taking the most significant shares of heat sectors of many nations (IRENA, 2017).

Unlike the geothermal production of electricity that requires high-temperature fluids (liquid water and vapour of over 125 °C) to power generation, unconventional low-temperature geothermal resources can provide energy to meet space and district heating applications (Jolie et al., 2021; Kukkonen, 2000). Geothermal energy is available evenly throughout the year, regardless of the weather, so it can form a basis for heating. For example, in Finland, geothermal energy has been researched since the 1970s, but the applications have been prevalently targeting shallow (<300 m) geothermal systems (Kukkonen, 2000), mainly using borehole heat exchangers (BHEs) and ground-source heat pumps (GSHPs) to deliver space heating for single-family dwellings. In the last 10 years, the share of larger installations has been increasing, as more efficient BHEs and GSHP systems are supplying heat for offices, industrial buildings, and residential blocks (Statistics Finland, 2021). Whereas shallow geothermal wells are likely to take a good share of future heat spacing markets (IRENA, 2017), in the urban areas, the challenge of shallow geothermal heat production is the lack of available surface land area required by large BHE field construction. Deeper BHEs use less land area and may offer more extractable energy per area, with higher fluid temperature outcome.

In the scientific literature, the terms medium-deep and deep borehole heat exchanger are used interchangeably, typically corresponding to an arbitrary depth of geothermal production. For example, in China and Central Europe, the depth limit for shallow borehole heat exchangers is defined as 200 m (e.g., Pan et al., 2020; Welsch, 2019), whereas in Northern Europe, conventional borehole heat exchangers can reach depths of 400 meters (Korhonen et al., 2019). For medium-deep geothermal boreholes, some authors have considered the depth of 3000 m (Chen et al., 2019; Pan et al., 2020), while others have suggested 1000 m as ideal boundaries (Holmberg, 2016; Schulte, 2016; Welsch, 2019). Here, we use the term medium-deep to describe geothermal systems with a range of depths of 600–3000 meters, based on our experience dealing with the emerging geothermal heat industry in Nordic countries. Irrespective of these depth markers, a common feature of medium-deep borehole technology is the integration of a coaxial heat collector to exchange heat from the host rock

to the fluid in the borehole (Cai et al., 2019; Kohl et al., 2002, 2000; Pan et al., 2020). In such a manner, the BHEs are designed to extract geothermal energy from the host rock by circulating the working fluid in a well without necessarily extracting fluids from the enclosing rock formation (Renaud et al., 2019).

To date, there are only a few medium-deep geothermal heat production boreholes in Europe. Commercial examples include two 1.5-km-deep boreholes installed to keep Oslo airport in Norway ice-free (Kvalsvik et al., 2019), and a medium-deep borehole operating in Weggis, Switzerland, which produces 220 MWh/a of heat for a residential area (Kohl et al., 2002). The highest peak power recorded for any medium-deep borehole produced near 400 kW of heat in a test of a 2 km deep borehole in Cornwall, UK (Collins and Law, 2014). In Finland, there is one pilot 1300-m-deep well under test using a coaxial heat collector near Helsinki and four systems are in the drilling phase across the country. Conversely, some commercial failures have also been reported, such as the Aachen SuperC project in Germany, which experienced several technical issues with plastic pipes, resulting in a maximum recovery temperature of 35 ºC (Falcone et al., 2018).

Here, we investigate the effects of multiple geological and engineering variables in the heat outcome of medium-deep geothermal boreholes. We apply a numerical finite element method to model how the interplay of thermogeological, climatological and engineering parameters affects the geothermal well performance. The input data relies on verified measurements and best practices of energy and drilling companies. We selected three locations in different parts of Finland to estimate how their geological and climatological parameters influence the outcome productivity of geothermal energy wells at different depths. Our work aims to answer three fundamental topics that will leverage the exploration of geothermal systems in crystalline rocks in Finland and globally: (i) How medium-deep geothermal energy production is affected by the underlying geological and climatological conditions? (ii) How much energy is possible to obtain by drilling deeper, and what are the outlet temperatures of medium-deep BHE systems compared to the production of shallow BHEs systems? and (iii) Is there a relevant performance difference between medium-deep BHEs heat collector types? Our resulting models will increase the likelihood of locating and designing profitable medium-deep geothermal systems in crystalline rocks, scaling-up the existing low-carbon solutions for the heating sector.

Geological and geothermal setting

Finland is located in the central Fennoscandian Shield, characterized by a cold and thick lithosphere (Grad et al., 2014). The age of the crystalline bedrock varies from Archean (3100–2500 Ma) to

Proterozoic (2500–1200 Ma), comprising of rocks formed by multiple tectonic plate collisions and continental terrain accretions (Nironen et al., 2017). The Precambrian bedrock of Finland is covered by a continuous, thin layer of glacial and postglacial sediment deposited during the Weichselian glacial stage and the Holocene, varying in thickness from a few metres to some tens of metres (Lahermo et al., 1990; Lunkka et al., 2004). Typically, the average thermal conductivity of crystalline rocks in Finland is around 3.2 W/(m·K), depending mainly on their mineral composition (Peltoniemi and Kukkonen, 1995). The geothermal gradient of Finland varies between 8-17 K/km and the mean annual ground temperature is controlled by climatological conditions, varying from +7 °C in Southern Finland to +1 °C in the northern parts of the country (Aalto et al., 2016).

Our study focuses on three areas across Finland: (i) Vantaa, (ii) Jyväskylä, and (iii) Rovaniemi, aiming to obtain information on the potential of medium-deep geothermal heat production in different geothermal settings in the southern, central, and northern Finland, respectively (Figure 1). Vantaa area comprises Paleo-to-Mesoproterozoic granitoids and high-grade metamorphic rocks, much of with has experienced intense partial melting (i.e., migmatization) during the Svecofennian Orogeny (Korsman et al., 1997). Granitic rocks in Vantaa often have a high percentual of microcline minerals, conferring a potassium-rich composition and consequently high radiogenic heat production properties. However, remanent of older felsic and ultramafic rocks can occur in the Vantaa area, forming a heterogeneous crustal block (Nironen, 2005). Jyväskylä area, as Vantaa, also sets with the Svecofennian tectonic province. However, most rocks in the Jyväskylä region are part of the Central Finland Granitoid Complex, a crustal block characterized by syn- and post-kinematic tonalites, granodiorites, quartz montzonites and granites that provide the lowest radiogenic heat production properties examined in this study. In contrast, Rovaniemi area is part of the Karelian tectonic province, characterized by the Central Lapland Granite Complex in the north and by the Paleoproterozoic Peräpohja Schist Belt in the south (Nironen, 2005). Rocks in Rovaniemi have a complex interrelationship between porphyritic granites, granodiorites, gneissic inclusions and various migmatitic bodies that give relatively high radiogenic heat production properties (Nironen et al., 2017).

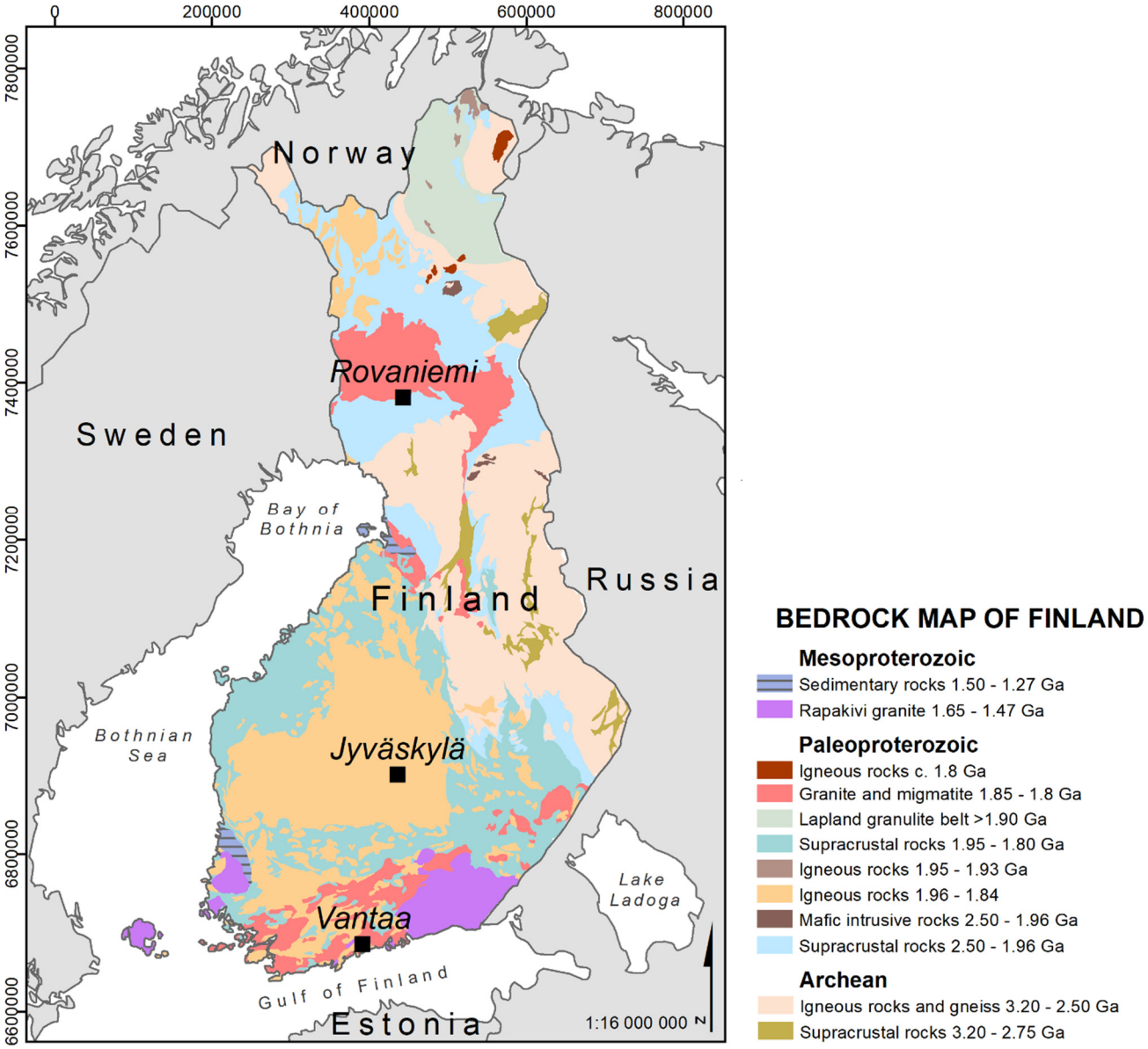

Fig. 1: Regional geological map of Finland showing the study area location. Adapted from Bedrock of Finland 1:5.000.000.

Materials and methods

Thermogeological parameters

To estimate the potential of medium-deep geothermal systems in Finland, we use both data primarily obtained from the literature and information derived from these original datasets (Table 1). The mean annual ground temperatures (T_g) were calculated using the relationship suggested by Kukkonen (1986):

$$T_g = 0.71 \cdot T_a + 2.93 \quad (1)$$

where T_a is the mean annual air temperatures for the climatological normal period 1931–1960 from the data of the Finnish Meteorological Institute (Aalto et al., 2016). The cell size of the mean annual

air temperature data is 1 km^2. The geological map is adapted from the digital Bedrock map of Finland at the scale of 1:5M (Figure 1). Each lithological unit was assigned a thermal conductivity value based on laboratory measurements presented by Peltoniemi and Kukkonen (1995). Radiogenic heat production rates (A_0) were compiled from Veikkolainen and Kukkonen (2019). Radiogenic heat production rate is based on equation from Rybach (1973):

$$A_0 = \rho \cdot (9.52 \cdot c_{\mathrm{U}} + 2.56 \cdot c_{\mathrm{Th}} + 3.48 \cdot c_{\mathrm{K}}) \cdot 10^{-5} \quad (2)$$

where ρ is rock density and c the concentration of U, K and Th. Further, we estimated the geothermal heat flux from the radiogenic heat production rates described above, using Birch's law,

$$q = q_0 + DA_0 \quad (3)$$

where q_0 is the reduced heat flux density (the heat flux density below the heat-producing crustal layer), D is the thickness of the heat-producing crustal layer, and A_0 is the near-surface radiogenic heat production rate (Eppelbaum et al., 2014). Veikkolainen and Kukkonen (2019) calculated the coefficients q_0 and D by fitting Eq. (3) to paleoclimatically corrected heat flux data, resulting in the reduced heat flux density of 33.79 mW/m^2 and the thickness of the heat-producing crustal layer of 5.919 km.

Rock density was assigned a constant value of 2725 kg/m^3 based on the averaging lithology of the study areas, as constrained density calculated by Pirttijärvi et al. (2013) and specific heat capacity of the rock at each location was assigned a constant value of 728 J/kg·K based on laboratory measurements conducted on Finnish rock samples by Kukkonen (2015).

Table 1: Thermogeological parameters of each location investigated in this study.

	Rovaniemi	Jyväskylä	Vantaa	Source
Mean annual air temperature [°C]	0.89	3.38	4.51	Aalto et al., 2016
Mean annual ground temperature [°C]	3.6	5.3	6.1	Calculated from air temperatures using Eq. (1)
Rock type	Porphyritic granite	Granodiorite	Microcline granite	Digital geological map of Finland 5M (GTK database)
Thermal conductivity of bedrock [W/(m·K)]	3.30	3.19	3.30	Peltoniemi and Kukkonen, 1995
Radiogenic heat production [μW/m^3]	2.56	1.33	2.96	Veikkolainen and Kukkonen, 2019

Geothermal heat flux [mW/m^2]	42.8	44.0	44.5	See text for calculation procedure
Geothermal gradient [K/m]	13.0	13.9	13.5	Calculated by dividing the geothermal heat flux density by the bedrock thermal conductivity

Borehole design, heat exchangers, and heat collector pipes

We model borehole heat exchangers of four lengths: 600, 1000, 2000, and 3000 meters (Fig. 2). In the 600 meters U-tube model, the working fluid was an ethanol–water mixture with 28 wt% ethanol. In the coaxial BHE models, water was used as the heat carrier fluid. The topmost 300 meters of the boreholes were cased to avoid any exchange with the shallow environment. Typically, crystalline rocks have low natural permeability, and the groundwater can only enter a borehole if it intersects a fracture zone. We assume that the boreholes do not intersect any permeable zones deeper than 300 m, so the deeper part of the borehole was left uncased, and the working fluid of the coaxial models was in direct contact with the bedrock below the casing. Casing the top part of the borehole prevents cool groundwater from entering the borehole, but the low thermal conductivity of the concrete casing acts as an insulator, so leaving most of the borehole uncased allows more efficient heat transfer between the bedrock and the working fluid. The present modelling options, including the casing procedure, are based on the suggestions and the interest of industry and companies operating in Finland.

We compared two types of collector pipes: vacuum-insulated tubing (VIT) and standard high-density polyethylene (HDPE) pipe. The most important parameter that distinguishes these two pipe types is their thermal conductivity. VIT consists of two concentric steel pipes separated from each other by vacuumed-air space. Effective thermal conductivity of 0.02 W/m·K was used for the VIT in this study (Śliwa et al., 2018; Zhou et al., 2015). As an industrial standard, HDPE pipes have higher thermal conductivity of 0.42 W/m·K. However, HDPE is still in use because of its significantly lower price ((Chen et al., 2019; Saaly et al., 2014). The efficiency of the VIT was experimentally tested in, for example, Weggis, Switzerland (Kohl et al., 2002), and HDPE pipes have been modelled by Wang et al., (2017).

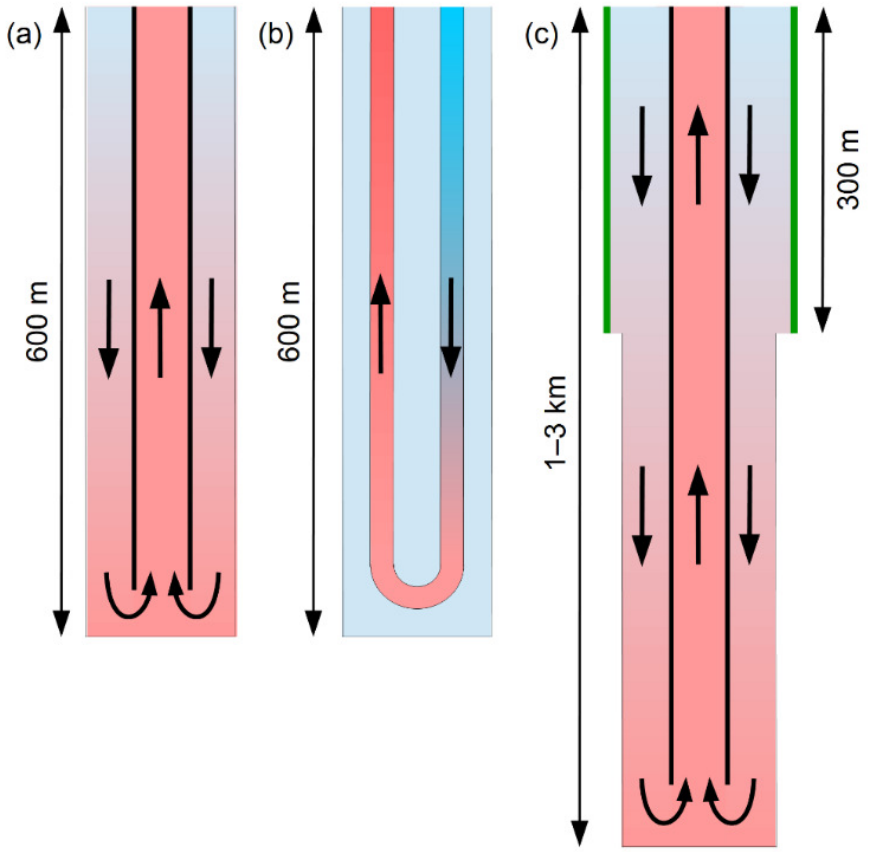

Fig. 2: The borehole heat exchangers modelled in this study. (a) A 600-m-deep open-loop coaxial borehole heat exchanger, (b) a 600-m-deep U-tube borehole heat exchanger, and (c) a 1–3-km-deep open-loop coaxial borehole heat exchanger with casing on the topmost 300 meters (green). Arrows indicate the direction of working fluid circulation.

For the 1–3-km-deep BHEs, we considered the boreholes to have a diameter of 8.5 inches (215.9 mm). The topmost 300 meters of the wellbores were 12.25 inches (311 mm) in diameter and were cased with 33-mm-thick cement casing. The 600-m-deep coaxial BHE was uncased, and its diameter was 160 mm. For the 600-m-deep BHEs, two diameter options for the VIT and one for the HDPE pipe were considered. As a comparison, we also modelled a standard U-tube BHE with a HDPE collector, an existing and tested BHE system. All BHE parameters were chosen based on existing or planned pilot experiments in Finland, and the parameters are summarized in Table 2.

The maximum volumetric flow rate was separately determined for each borehole depth based on the pressure loss in the well calculated with Moody friction factor approximation for smooth pipes,

$$f = \begin{cases} 0.316 \cdot Re^{-1/4} & \text{if } Re \leq 20{,}000 \\ 0.184 \cdot Re^{-1/5} & \text{if } Re > 20{,}000 \end{cases} \quad (4)$$

where Re is the Reynolds number, calculated as $Re = uD/\nu$, where u is the mean fluid velocity in the pipe, D is the inner pipe diameter and n is the kinematic viscosity of the fluid (Incropera and DeWitt, 1996). The pressure loss in the pipe was calculated using

$$\Delta p = \frac{fLu^2}{2D} \quad (5)$$

where L is the pipe length and u is the velocity of the fluid in the pipe. Pipe roughness and minor losses caused by velocity changes in the pipe diameter changes, well bottom, valves, etc. were considered to have little impact on the total pressure loss and consequently were not assessed in detail. The acceptable pressure drop was set as 2 bars for 1-km pipes, 4 bars for 2-km pipes and 5 bars for 3-km pipes. In the case of 600-m pipes, the increase in flow rate was dictated by temperature losses more than by pressure losses, and the maximum volumetric flow rate was therefore set to 3 L/s.

Table 2: Summary of borehole heat exchanger parameters adopted in this study. All borehole and pipe diameter values are from the Drilling data handbook (Gabolde et al., 1999).

1. Borehole depth (m) and type	600, U-tube	600, coaxial	1000, coaxial	2000, coaxial	3000, coaxial
2. Borehole diameter (mm)	160	160	0 – 300 m: 311; 300 – 1000 m: 215.9	0 – 300 m: 311; 300 – 2000 m: 215.9	0 – 300 m: 311; 300 – 3000 m: 215.9
3. Collector thermal conductivity (W/(m*K))	HDPE, k = 0.42	VIT, k = 0.02	VIT, k = 0.02	VIT, k = 0.02	VIT, k = 0.02
		HDPE, k = 0.42	HDPE, k = 0.42	HDPE, k = 0.42	HDPE, k = 0.42
4. Collector inner/outer diameter (mm)	51.4/63	VIT, 50/89	VIT, 76/114	VIT, 76/124	VIT, 76/124
		VIT, 76/114			
		HDPE, 80/100	HDPE, 100/120	HDPE, 100/120	HDPE, 100/120
5. Casing length and thickness	No	No	300 m, 33 mm	300 m, 33mm	300 m, 33 mm
6. Flow rate (L/s)	1–3	1–3	1–5	VIT, 1–5	VIT, 1–5
				HDPE pipe, 2–10	HDPE pipe, 2–10

Numerical modelling

The finite element modelling and simulation platform COMSOL Multiphysics® was used to construct the models of the BHEs illustrated in Figure 2 and to simulate their operation. The open-loop coaxial BHEs were modelled using two-dimensional axisymmetric models and the U-tube BHE was modelled using a three-dimensional model. The equation used to describe the temperature field T was

$$\rho C_p \frac{\partial T}{\partial t} - k\nabla^2 T + \rho C_p \mathbf{u} \cdot \nabla T - A_0 = 0, \quad (6)$$

where t is time, ρ is density, C_p is the specific heat capacity, k is thermal conductivity, $\mathbf{u}$ is velocity vector, and A_0 is the radiogenic heat production rate. All models comprised domains representing the piping, working fluid, and rock, together with casing when included. Furthermore, the working fluid was assumed to instantaneously conduct heat horizontally to simulate turbulent flow.

The boundary conditions applied to the model were the surface geothermal heat flux density estimated using Birch's law (Equation 3) at the ground surface boundary and the reduced geothermal heat flux density at the bottom boundary of the model. Heat extraction was assumed to be constant throughout the year, which corresponded to a heat pump dropping the entering water temperature (T_{ewt}) by

$$\Delta T = \frac{E_{\mathrm{ann}}}{H} \cdot \frac{1}{\rho C_p Q} \quad (8)$$

where E_{ann} is the amount of heat annually extracted from the ground, H is the number of hours in a year (8760 h), rC_p is the volumetric heat capacity of the working fluid, and Q is its flow rate. Thus, the leaving water temperature was $T_{\mathrm{lwt}} = T_{\mathrm{ewt}} - \Delta T$ and was imposed as a temperature boundary condition on the BHE inlet.

Solving maximal annual energy yield

COMSOL Multiphysics® was used to simulate 25 years of operation of the BHEs systems. A COMSOL simulation was expressed as

$$f(\boldsymbol{\theta}; E_{\mathrm{ann}}) = T_{\mathrm{min}} \quad (9)$$

where f is a function that maps the vector of model parameters $\mathbf{q}$ and annually extracted energy E_{ann} to T_{min}, which is the minimum temperature at the borehole wall at the end of the simulation. The maximal amount of thermal energy E_{max} that can be extracted annually from the ground using a BHE without dropping the borehole outer boundary temperature below the freezing point of 0 °C was determined by solving

$$E_{\mathrm{max}} = \arg\min_{E_{\mathrm{ann}}} |f(\boldsymbol{\theta}; E_{\mathrm{ann}})| \quad (10)$$

The minimization problem in Eq. (10) was solved for each location, borehole length, collector type, and volumetric fluid flow rate using MATLAB® and COMSOL through LiveLink™ for MATLAB. In this study, the energy values are pure geothermal heat from the subsurface, and additional energy from running the heat pumps is not assessed. Therefore, our results provide a first-order estimation of the amount of thermal energy from each location.

Results

Energy production estimation

The energy production estimation was based on different geological and borehole designing parameters (Tables 1-2). Our models indicate that the thermal energy yield is highest in the southernmost Vantaa area (up to 1880 MWh/a), slightly lower in central Finland Jyväskylä (up to 1830 MWh/a), and lowest in the northernmost Rovaniemi location (up to 1590 MWh/a) (Table 3). In Rovaniemi, the thermal energy yield is 15–26% lower than in Vantaa, and 13–18% lower than in Jyväskylä. In addition, the thermal energy yield of each location is directly proportional to the borehole depth. We observe that as the BHE depth increases from 600 to 1000 m, the thermal energy yield roughly doubled, nearly tripled from 1000 to 2000 m, and almost doubled when increasing the depth from 2000 to 3000 m. These results show that the BHE energy production can increase over 10-fold from 600 to 3000 m depth.

Table 3: Maximum thermal energy production (MWh/a) from three locations with VIT pipe and a flow rate of 3 L/s with a 600-m-deep well and 5L/s with well depths of 1000 m, 2000 m, and 3000 m.

Well depth (m)	Vantaa (MWh/a)	Jyväskylä (MWh/a)	Rovaniemi (MWh/a)
600	170	150	125
1000	330	310	270
2000	980	950	830
3000	1880	1830	1590

At the highest used volumetric flow rates, the energy yield does not depend on the pipe type (Fig. 3a). With 600-1000 m deep wells, the working fluid outlet temperature is 1.2–2 °C (northern to southern location) regardless of the collector type (Fig. 3b). As the borehole depth increases to 2 and 3 km, outlet temperatures attained with VIT are twice as high as those with HDPE pipes. At a depth of 3 km, the VIT temperatures achieved 8.7–10 °C, whereas HDPE pipes can only produce 4.2–5 °C, i.e., half of the VIT heat outcome. With an increase in borehole depth from 1 km to 2 km, the specific heat rate increases from 31–35% with VIT and 30–50% with HDPE pipe, depending on the location

(Fig. 3c). The specific heat rate of both collectors grows around 14–20% when the borehole depth increases from 600 m to 1 km, and 20% when the borehole depth increases from 2 to 3 km.

At the lowest modelled volumetric flow rates, the increase in the energy yield as a function of depth is linear with VIT, which rises by a factor of 1.8 between 600 m and 1 km, 2.4 between 1 and 2 km, and 1.5 between 2 and 3 km (Fig. 3d). With HDPE pipe, the energy yield remains practically the same between 600 m and 1 km but increases by a factor of 3.3 when the borehole depth increases from 1 to 2 km, and again by only 1.2 when deepening the borehole from 2 to 3 km. Differences in the working fluid outlet temperature depending on the collector type are more evident at low flow rates. In the VIT case, the 600-m-deep well outlet temperature increases linearly from 3–3.9 °C (northern to southern), and respectively from 23–27 °C using a 3-km-deep borehole. With HDPE pipe, the 600-m deep well outlet temperature increases linearly from 2.4–3 °C, and to 6.6–7.9 °C in a 3-km-deep well (Fig. 3e). With VIT, the specific heat rate increases by 7–15% between 600 m and 1 km, 13–20% between 1 and 2 km, and less than 10% between 2 and 3 km. With HDPE pipe, the specific heat rate decreases by 28–36% between 600 and 1000 m, increases 40% between 1 and 2 km, and decreases again 20% between 2 and 3 km (Fig. 3f).

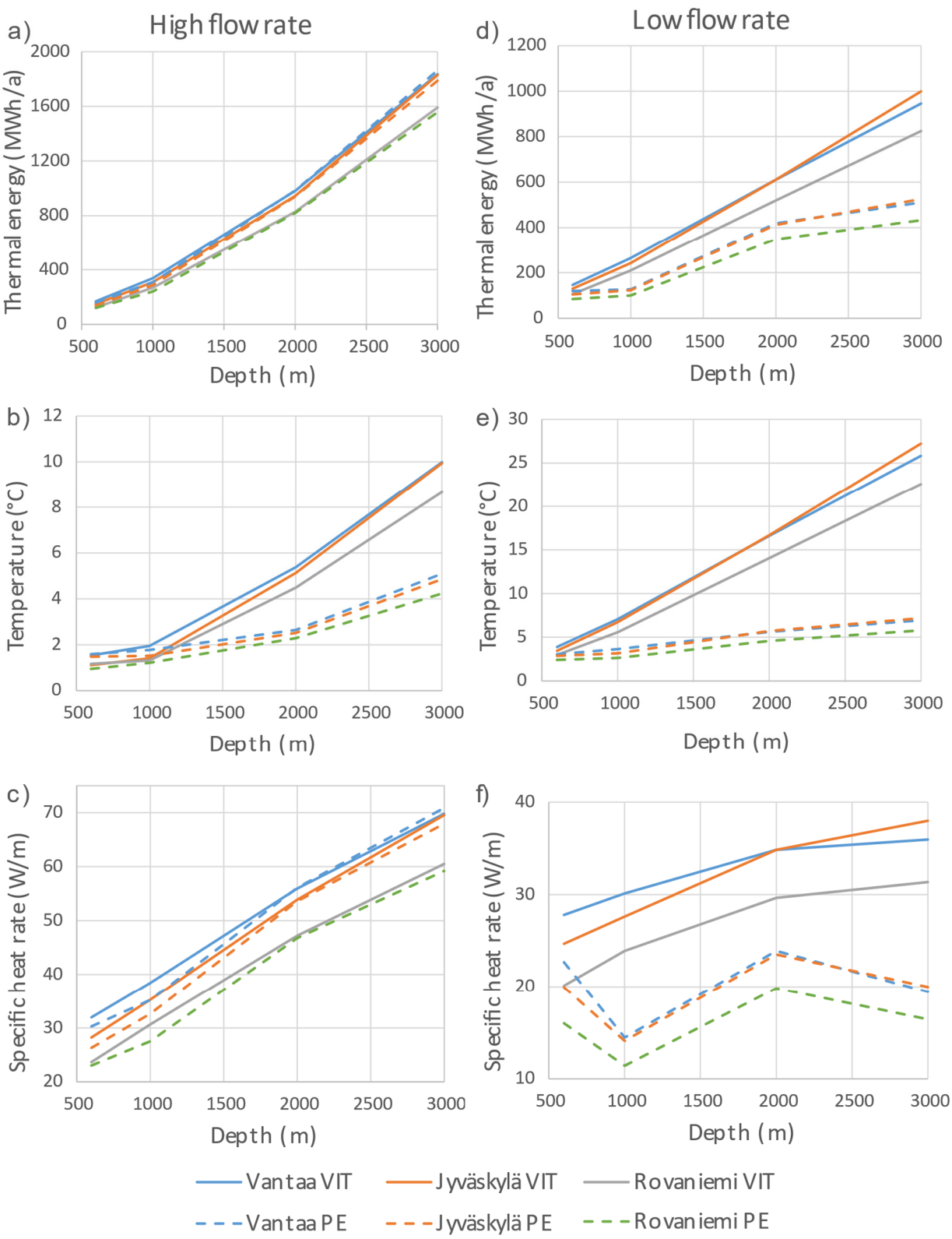

Fig. 3: Comparison of thermal energy produced by constant heat extraction over 25 years, with the outlet temperature and specific heat rate at high and low flow rates for each modelled depth, location, and two collector pipe types. The highest flow rates for VIT are 5 L/s at all pipe lengths, while for HDPE pipe they are 5 L/s at 1 km and 10 L/s at 2 km and 3 km. The lowest flow rates are 1 L/s for VIT at all pipe lengths and for 1 km of HDPE pipe, and 2 L/s for 2 km and 3 km HDPE pipe.

Effect of thermal short-circuiting

The effects of the pipe material and fluid flow rate circulation are crucial for understanding the performance of medium-deep BHEs. We observe that a 2-km-deep well with VIT produces 980 MWh/a at highest circulation rates (5 L/s). To obtain the same amount of thermal energy, the flow rate in HDPE pipe needs to be doubled. With these energy production values, VIT yields an outlet temperature of 5.4 °C, while HDPE pipe yields 2.6 °C. The vertical profiles of a 2-km-deep BHE from Vantaa from the 25-year production simulation at different flow rates are presented in Figure 4. As a comparison, if the flow rate in HDPE pipe is lower, the temperature increases towards the bottom of the borehole and decreases again as fluid returns to the surface (Figure 4, blue, green, and red lines). This temperature difference reflects the thermal short-circuiting effect, and the lower the volume flow is, the greater is the effect. Thermal short-circuiting is observed at a much smaller scale in the vertical profile of VIT with a flow rate of 1 L/s (Figure 4, black line), while at high flow rate there are practically no heat losses in the inner pipe (Figure 4, grey line).

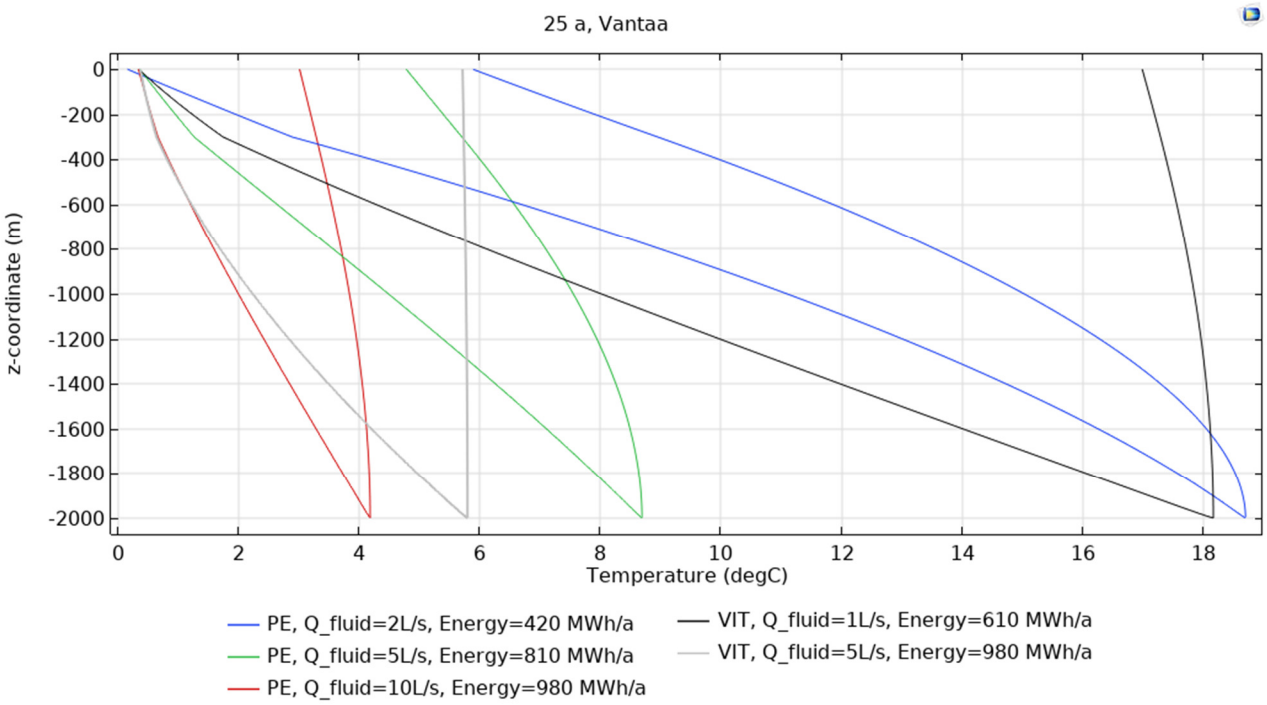

Fig. 4: Vertical temperature profiles of a 2000-m BHE with a VIT or HDPE pipe collector and different volumetric flow rates

System efficiency as a function of production time

Our models show that the outlet temperature drastically drops during the first days of utilization of the geothermal systems, and then slowly decrease over time (Figure 5). After one year (close-up in Figure 5), we see that after the initial drop, temperature begins to stabilize but is still 2–5 °C higher after the first year of production than at the 25th production year. For all flow rates and collector cases, inlet temperatures drop to 0 °C after 25 years, as the model optimization parameters require.

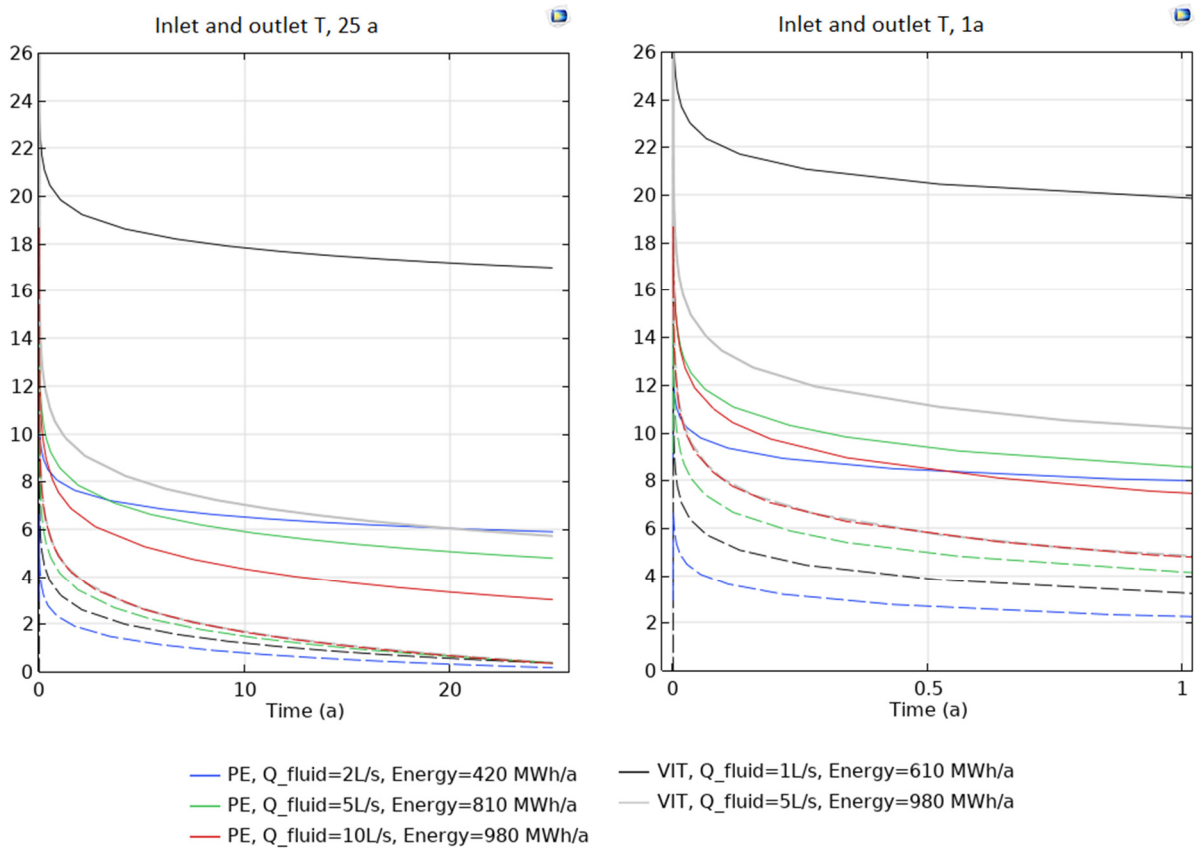

Fig. 5: Outlet (solid line) and inlet (dashed line) temperatures of a 2000-m BHE with VIT or HDPE pipe and different volumetric rates. The left figure presents temperature development over 25 years of simulation and the figure on the right is a close-up of the first year of production.

600-m-deep wells

Parametrization of the 600-m-deep BHE was conducted with four different collector pipes, so the results for thermal energy production and the outlet temperature as a function of flow rate are presented here separately, only including results from the southernmost Vantaa area. The smaller diameter VIT pipe outperforms the other pipes in thermal energy production, regardless of the flow rate, but HDPE pipe performs better in terms of the outlet temperature at the highest flow rate of 3 L/s (Figure 6). The thermal energy yield is low with the U-tube, but the poorest yield and lowest outlet temperature are obtained with a larger diameter VIT.

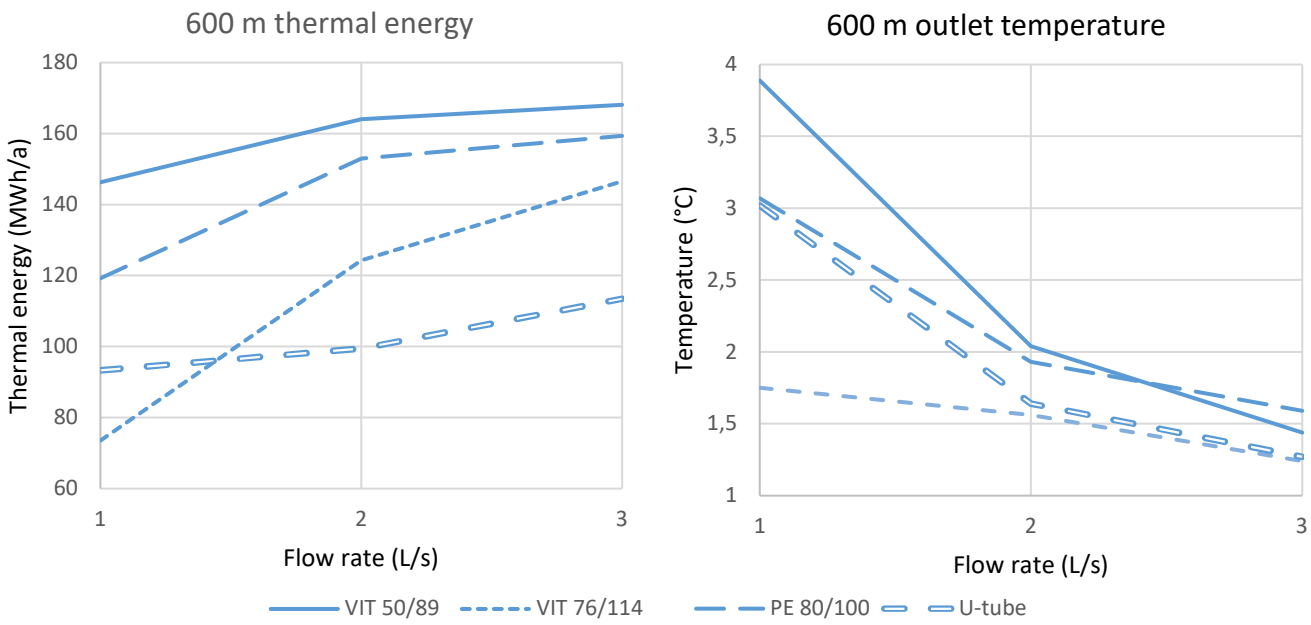

Fig. 6: Thermal energy and outlet temperature from 600 m wells as a function of flow rate with four different collectors.

Discussion

Geological and climatological influence on geothermal production

The lowest ground temperature levels and consequently the lowest thermal energy yield is observed in Rovaniemi, the northernmost location. The highest thermal energy yield is observed in the southernmost location, Vantaa, as a result of the three factors: the highest ground surface temperature, high geothermal heat flux density, and high radiogenic heat production values due to the presence of microcline granites. The geothermal gradient in Jyväskylä is higher than in the two other locations due to the lower thermal conductivity and radiogenic heat production, so in both Jyväskylä and Vantaa, the temperature reaches 13.4 °C at a depth of 600 m, while at greater depths, the temperature is higher in Jyväskylä than in Vantaa. Regardless of the higher geothermal gradient in Jyväskylä, the outlet temperatures and thermal energy yield are mainly lower than in Vantaa. This difference in outlet temperature is attributed to the lower thermal conductivity of the granodiorite than microcline granite and consequently less efficient heat exchange between the host rock and the fluid.

Compared to other locations where deep geothermal wells have been drilled or modelled, Finland typically has lower heat flow and geothermal gradient, and therefore our models generally result in either lower outlet temperatures or thermal power. Chen et al. (2019) modelled a 2.6-km borehole in the “standard” and “elevated” geothermal gradient of 30 and 40 K/km, respectively and their models resulted in the specific heat rate of 125–200 W/m. Correspondingly, our specific rates for a geothermal gradient of 13-14 K/km are 50 W/m for a 2-km well and 70 W/m for a 3-km well –

approximately 0.4 of the values reported by Chen et al. (2019). The simulated values of 886–1129 MWh/a for the 2.1-km-deep well in Weggis, Switzerland (Kohl et al., 2002) correlate with our results for a 2-km-deep borehole. In Weggis, the temperature recorded at the bottom of the 2.3-km-deep well was 73 °C (Kohl et al., 2002), which is roughly double than that in Jyväskylä, but their simulated energy yield values correlate with our results because the volumetric flow rate used in Weggis was lower than in our study.

As a conclusion, we observe that initial ground surface temperature and consequently the geothermal gradient have a significant impact on geothermal energy yield, while thermal conductivity of the local rock type has a more complex impact that depends on the production properties such as fluid flow rate. This is apparent from the comparison of the results obtained in thermogeological settings of Switzerland and Finland, as well as from the results of our study comparing thermogeological variations across Finland. Another essential finding is that, as the borehole depth increases from 600 to 1000 m, the thermal energy yield roughly doubled, nearly tripled from 1000 to 2000 m, and almost doubled when increasing the depth from 2000 to 3000 m.

Collector type and flow rate

Our models suggest that the efficient insulation of VIT pipes allow thermal energy production comparable with HDPE pipes with large hydraulic diameter and consequently higher flow rates (Figure 3, Table 2). This relationship between flow rate and types of pipes is an essential finding if we consider that HDPE pipe is significantly lower in price than VIT. However, the fluid temperatures produced with HDPE pipe are relatively low at all flow rates and borehole lengths due to the thermal short-circuiting effect, being at their highest around 8 °C from a 3-km-deep well at a low volumetric flow rate (2 L/s). On the other hand, fluid outlet temperatures produced with VIT at low flow rates are 2.5–3 times higher than temperatures produced with either HDPE pipe or VIT with high flow rates.

The results of this study are similar to those in previous publications based on medium-deep wells in Nordic countries. Holmberg (2016) observed that borehole depth significantly affects the heating power, with the yield increasing by 8-fold when borehole length was increased from 300 m to 900 m. The power produced from a 600-m-deep well was on average 30 kW and that from a 1000-m-deep well was on average 65 kW (Holmberg, 2016), corresponding to 263 MWh/a and 569 MWh/a, respectively. In addition, the energy yield from a reference 2-km-deep borehole was 1 GWh/a over 25 years (Lund, 2019). We estimate that the energy yields presented in Holmberg (2016) are higher due to the short simulation time of 5000 h (208 days). When heat outtake is optimized for a more extended period, less annual heat production is expected. This reduction in extractable heat as a

function of time was demonstrated by Lund (2019), in which energy extracted during the first 5 years was 1.2 GWh/a, dropping to 1 GWh/a when averaged over 25 years. The main reason for the higher yield in the latter case is the higher volumetric flow rate.

We arrive at the same conclusion as Nalla et al. (2005) that either the thermal power production or the outlet temperature of working fluid can be individually maximized. Alternatively, they can be simultaneously optimized so that reasonable temperatures for heat pump(s) as well as a reasonable heat production rate can be expected. Therefore, a correct flow rate parametrization and efficient insulation of the heat collector become essential at large-scale medium-deep geothermal systems. The slower the fluid flows in the borehole, higher temperature can be achieved, although less heat can be extracted. This effect is apparent in all the HDPE pipe results: the outlet temperature is generally lower and does not decrease as drastically with an increase in flow rate compared with VIT.

Comparison of medium-deep and shallow geothermal energy utilization

A common misconception of medium-deep wells is that they can produce long-term heating with high working fluid temperatures. Our models show that fluid outlet temperatures from 2 km boreholes can be up to 17 °C and from 3 km boreholes up to 27 °C (Figure 3e). In Finland, the typical outlet temperature from conventional shallow geothermal wells is around 0 - 4 °C (Korhonen et al., 2019), depending on the location and subsurface properties. In such small-scale closed-loop systems, the ethanol-based heat carrier fluid heats up by 1-3 degrees on average during heat extraction. By drilling deeper, we reach higher ground temperature levels, and the heat carrier fluid is consequently expected to warm up more. The advantages sought from medium-deep wells over shallow geothermal wells are related to two scenarios: 1) maximizing heat production with high flow rates and lower ground area requirements compared with conventional BHE fields; or 2) obtaining a higher return fluid temperature with low flow rates, which allows heat production coupled with a heat pump having good efficiency and thus heat distribution at a higher temperature than conventional BHE systems.

Related to the first scenario, we can subsequently compare the specific heat rate between medium-deep and shallow boreholes from the potential of shallow geothermal energy reported by Arola et al. (2019). According to a shallow geothermal energy potential dataset produced by the Geological Survey of Finland, a single 300-m-deep borehole has a constant thermal power of 7632 W (25 W/m) in Vantaa, 5887 W (20 W/m) in Jyväskylä and 5320 W (18 W/m) in Rovaniemi. A 1-km-deep borehole with VIT at a high flow rate can produce a specific heat rate of 30–38 W/m, while the respective figures for a 2- and 3-km-deep borehole are 47–56 W/m and 60–70 W/m (Figure 3). The achievable specific heat rate of a medium-deep borehole is therefore higher than what can be extracted from conventional shallow BHE systems, but this is predominantly valid at high flow rates. At low

flow rates, the increase in the specific heat rate is smaller. With HDPE pipe, the specific heat rate is highest with 2-km-deep wells, where it is between 20–25 W/m, thus corresponding to the energy extractable from conventional shallow systems. With 1- and 3-km-deep wells, the specific heat rate is lower than conventional shallow systems. When comparing the specific heat rates between medium-deep and shallow boreholes, one must bear in mind that in shallow closed-loop systems, U-tubes are the dominant technology, and the volumetric flow rates are lower.

Further considerations

Considering the temperature levels presented in this study, a heat pump is needed to raise the resulting temperature to the level required by the property or district heating system. District heating can be realized as low-temperature heating, to which medium-deep geothermal energy is well suited (Schmidt et al., 2017). A constant energy outtake was chosen to calculate the baseload that geothermal heat could provide, but intermittent energy outtake could provide a higher peak power (E.g., Kohl et al., 2002), while the recharging of wells with, for example, waste or solar heat could not only provide a higher yield but also prolong the well lifetime. Therefore, further optimization of any geothermal system should be done taking into considerations case-specific characteristics, such as the end use (local or district heating), required peak power and availability of rechargeable heat in the form of waste heat or solar collectors.

Questions that must be investigated in further work include a sensitivity study on a wider range of subsurface properties and BHE parameters, such as borehole and collector dimensions and the impact of different casing materials. The parameters for the present study were purely based on the geographical location and pipe parameters used in pilot projects or considered as industrial alternatives presently available in the market. Besides the highest thermal energy yield and highest possible production temperature, the CAPEX and OPEX costs of medium-deep geothermal systems are another essential factor to consider among stakeholders. For example, while VIT outperforms HDPE pipes in temperature production, it might still be more cost-effective to use HDPE or new innovative material solutions in the collector pipe. More detailed cost information may help estimate the amount of governmental financial support possibly needed to enable the geothermal industry to replace heating with fossil fuels with geothermal heat. Furthermore, an important task is to assess the accuracy of a model that only considers conductive heat transfer in the rock matrix, because it is likely that a well will intersect fracture zones may impact heat transfer in the formation and consequently in the borehole. Lastly, it is important to examine whether a seismic risk or other environmental risks are posed when installing medium-deep geothermal systems.

Conclusions

Exploration and production of medium-deep geothermal systems can significantly accelerate the transition away from fossil fuels by providing a clean and reliable energy source for residential and industrial heating. The results of this study indicate that: (1) the deeper the borehole is, the better is its thermal energy production and specific heat rate, (2) the higher the subsurface temperature, the better is the energy yield, when considering minor variations in thermogeological parameters, (3) VIT outperforms HDPE pipe in terms of energy and temperature production, and (4) with an increasing flow rate, we obtain more thermal energy but a significantly lower outlet fluid temperature. All these variables should be taken into consideration during the design and operation phases of medium-deep geothermal systems.

Drilling deeper may represent a viable option to increase the outcome of unconventional low-temperature geothermal systems in the district heating sector. Compared to shallow geothermal BHEs, medium-deep geothermal systems offer higher fluid outlet temperature that enables a higher coefficient of performance (COP) with a heat pump. Another advantage of deeper geothermal systems is that in densely populated areas, fewer wells will be needed to supply the same amount of heat, consequently having a smaller land surface impact than shallow geothermal systems. Our resulting models indicate that efficient medium-deep geothermal well operation must be carefully designed to suit the thermogeological parameters of the area. Understanding the interplay of these thermogeological and engineering parameters is critical to up-scale sustainable low-carbon geothermal systems in Finland and abroad where low permeability crystalline rocks dominate the geological setting.

List of symbols

Roman letters

A: radiogenic heat production (W/m^3); C_p: specific heat capacity at constant pressure (J/(kg·K)); c: concentration (ppm/‰); D: thickness (m); E: energy (MWh); f: Moody friction factor (dimensionless); H: number of hours in a year (dimensionless); k: thermal conductivity (W/(m·K)); L: length (m); p: pressure (Pa); q: geothermal heat flux density (W/m^2); Q: volumetric flow rate (L/s) Re: Reynolds number (dimensionless); t: time (s); T: temperature (°C); u: velocity (m/s); z: depth (m)

Greek letters

ρ: density (kg/m^3)

Subscripts

a: air; ann: annual; g: ground; in: inlet; K: potassium; max: maximum; min: minimum; out: outlet; Th: thorium; U: uranium; 0: initial

Declarations

Acknowledgements

The writers dedicate this work to M.Sc. (tech) Jarmo Kosonen who started the project but sadly passed away during the writing of this article. We acknowledge Matti Pentti and Kristian Savela from ST1 Ltd. and Risto Lahdelma from Aalto University for initial work and insightful help.

Authors' contributions

KP created the COMSOL model, run necessary computations and wrote the sections on borehole parameters, results, and co-wrote the introduction, discussion, and conclusion sections. AM wrote the sections on geology and co-wrote discussion and conclusion sections. SV and NL co-wrote the introduction and made valuable comments on the manuscript. KK wrote the sections on numerical modelling and solving for maximum annual energy yield and created the initial Matlab code applied in this study. TA and AB supervised the work and made valuable comments on the manuscript.

Funding

The project was partly funded by Business Finland's Smart Otaniemi subproject Smart integration of energy flexible buildings and local hybrid energy systems. Business Finland diary number: 52/31/2019.

Availability of data and materials

The datasets used and/or analysed during the current study are available from the corresponding author on request.

Competing interests

The authors declare that they have no competing interests.

References

Aalto, J., Pirinen, P., Jylhä, K., 2016. New gridded daily climatology of Finland: Permutation-based uncertainty estimates and temporal trends in climate. J. Geophys. Res. Atmos. 121, 3807–3823. https://doi.org/10.1002/2015JD024651

Arola, T., Korhonen, K., Martinkauppi, A., Leppäharju, N., Hakala, P., Ahonen, L., Pashkovskii, M., 2019. Creating shallow geothermal potential maps for Finland using finite element simulations and machine learning. Eur. Geotherm. Congr. 2019 6.

Cai, W., Wang, F., Liu, J., Wang, Z., Ma, Z., 2019. Experimental and numerical investigation of heat transfer performance and sustainability of deep borehole heat exchangers coupled with ground source heat pump systems. Appl. Therm. Eng. 149, 975–986. https://doi.org/10.1016/j.applthermaleng.2018.12.094

Chen, C., Shao, H., Naumov, D., Kong, Y., Tu, K., Kolditz, O., 2019. Numerical investigation on the performance, sustainability, and efficiency of the deep borehole heat exchanger system for building heating. Geotherm. Energy 7. https://doi.org/10.1186/s40517-019-0133-8

Collins, M.A., Law, R., 2014. The Development and Deployment of Deep Geothermal Single Well (DGSW) Technology in the United Kingdom, in: European Geologist. pp. 63–68.

Eppelbaum, L., Kutasov, I., Pilchin, A., 2014. Applied Geothermics, Endeavour, Lecture Notes in Earth System Sciences. Springer Berlin Heidelberg, Berlin, Heidelberg. https://doi.org/10.1007/978-3-642-34023-9

Falcone, G., Liu, X., Okech, R.R., Seyidov, F., Teodoriu, C., 2018. Assessment of deep geothermal energy exploitation methods: The need for novel single-well solutions. Energy 160, 54–63. https://doi.org/10.1016/j.energy.2018.06.144

Gabolde, G., Nguyen, J.-P., Gabolde, G., Nguyen, J.-P., Gabolde, G., 1999. Drilling Data Handbook. Ed. Tech. Paris.

Grad, M., Tiira, T., Olsson, S., Komminaho, K., 2014. Seismic lithosphere–asthenosphere boundary beneath the Baltic Shield. GFF 136, 581–598. https://doi.org/10.1080/11035897.2014.959042

Holmberg, H., 2016. Transient Heat Transfer in Boreholes with Application to Non-Grouted Borehole Heat Exchangers and Closed Loop Engineered Geothermal Systems. Doctoral thesis.

Holmberg, H., Acuña, J., Næss, E., Sønju, O.K., 2016. Thermal evaluation of coaxial deep borehole heat exchangers. Renew. Energy 97, 65–76. https://doi.org/10.1016/j.renene.2016.05.048

IEA, 2021. Global Energy Review 2021, Global Energy Review 2021. Paris.

Incropera, F.P., DeWitt, D.P., 1996. Fundamentals of Heat and Mass Transfer. https://doi.org/10.1016/j.applthermaleng.2011.03.022

IRENA, 2017. Renewable Energy in District Heating and Cooling: A Sector Roadmap for REmap, Int. Renew. Energy Agency. Abu Dhabi.

Jolie, E., Scott, S., Faulds, J., Chambefort, I., Axelsson, G., Gutiérrez-Negrín, L.C., Regenspurg, S., Ziegler, M., Ayling, B., Richter, A., Zemedkun, M.T., 2021. Geological controls on geothermal resources for power generation. Nat. Rev. Earth Environ. 2, 324–339. https://doi.org/10.1038/s43017-021-00154-y

Kohl, T., Brenni, R., Eugster, W., 2002. System performance of a deep borehole heat exchanger. Geothermics 31, 687–708. https://doi.org/10.1016/S0375-6505(02)00031-7

Kohl, T., Salton, M., Rybach, L., 2000. Data analysis of the deep borehole heat exchanger plant Weissbad (Switzerland). World Geotherm. Congr. 2000.

Korhonen, K., Leppäharju, N., Hakala, P., Arola, T., 2019. Simulated temperature evolution of large BTES – case study from Finland, in: Proceedings of the IGSHPA Research Track 2018. International Ground Source Heat Pump Association, pp. 1–9. https://doi.org/10.22488/okstate.18.000033

Korsman, K., Koistinen, T., Kohonen, J., Wennerström, M., Ekdahl, E., Honkamo, M., Idman, H., Pekkala, Y., 1997. Bedrock map of Finland 1: 1 000 000. Geol. Surv. Finland, Espoo, Finland.

Kukkonen, I., 2015. Thermal Properties of Rocks in Olkiluoto : Results of Laboratory Measurements 1994-2015. Posiva Work. Rep. 30, 110.

Kukkonen, I.T., 2000. Geothermal Energy in Finland. Proc. World Geotherm. Congr. 2000 277–282.

Kukkonen, I.T., 1986. The effect of past climatic changes on bedrock temperatures and temperature gradients in Finland, Geol. Surv. Finland, Nucl. Waste Dispos. Res. Espoo.

Kvalsvik, K.H., Midttømme, K., Ramstad, R.K., 2019. Geothermal Energy Use, Country Update for Norway, in: European Geothermal Congress 2019, Den Haag, The Netherlands, 11-14 June. den Haag.

Lahermo, P., Ilmasti, M., Juntunen, R., Taka, M., 1990. Suomen geokemian atlas, osa 1: Suomen pohjavesien hydrogeokemiallinen kartoitus, The geochemical atlas of Finland, Part 1: The hydrogeochemical mapping of Finnish groundwater.

Lund, A., 2019. Analysis of deep-heat energy wells for heat pump systems. Master's thesis 574–578. https://doi.org/10.1109/ISGT-Europe47291.2020.9248748

Lunkka, J.P., Johansson, P., Saarnisto, M., Sallasmaa, O., 2004. Glaciation of Finland, in: Developments in Quaternary Science. Elsevier Ltd, pp. 93–100. https://doi.org/10.1016/S1571-0866(04)80058-7

Nalla, G., Shook, G.M., Mines, G.L., Bloomfield, K.K., 2005. Parametric sensitivity study of operating and design variables in wellbore heat exchangers. Geothermics 34, 330–346. https://doi.org/10.1016/j.geothermics.2005.02.001

Nironen, M., 2005. Proterozoic orogenic granitoid rocks. Precambrian Geol. Finl. – Key to Evol. Fennoscandian Shield 14, 443–479. https://doi.org/10.1016/S0166-2635(05)80011-8

Nironen, M., Luukas, J., Kousa, J., Vuollo, J., Holtta, P., Heilimo, E., 2017. Bedrock of Finland at the scale 1:1 000 000 – Major stratigraphic units, metamorphism and tectonic evolution, Geol. Surv. Finland, Spec. Pap.

Pan, S., Kong, Y., Chen, C., Pang, Z., Wang, J., 2020. Optimization of the utilization of deep borehole heat exchangers. Geotherm. Energy 8, 6. https://doi.org/10.1186/s40517-020-0161-4

Peltoniemi, S., Kukkonen, I., 1995. Kivilajien lämmönjohtavuus Suomessa: yhteenveto mittauksista 1964-1994 14.

Pirttijärvi, M., Elo, S., Säävuori, H., 2013. Lithologically constrained gridding of petrophysical data. Geophysica 49, 33–51.

Renaud, T., Verdin, P., Falcone, G., 2019. Numerical simulation of a Deep Borehole Heat Exchanger in the Krafla geothermal system. Int. J. Heat Mass Transf. 143, 118496. https://doi.org/10.1016/j.ijheatmasstransfer.2019.118496

Rybach, L., 1973. Wärmeproduktionsbestimmungen an Gesteinen der Schweizer Alpen.

Saaly, M., Sinclair, R., Kurz, D., 2014. Assessment of a Closed-Loop Geothermal System for Seasonal Freeze-Back Stabilization of Permafrost.

Schmidt, D., Kallert, A., Blesl, M., Svendsen, S., Li, H., Nord, N., Sipilä, K., 2017. Low Temperature District Heating for Future Energy Systems. Energy Procedia 116, 26–38. https://doi.org/10.1016/j.egypro.2017.05.052

Schulte, D., 2016. Simulation and Optimization of Medium Deep Borehole Thermal Energy Storage Systems. Doctoral dissertation.

Śliwa, T., Kruszewski, M., Zare, A., Assadi, M., Sapińska-Śliwa, A., 2018. Potential application of vacuum insulated tubing for deep borehole heat exchangers. Geothermics 75, 58–67. https://doi.org/10.1016/J.GEOTHERMICS.2018.04.001

Statistics Finland, 2021. Energy in Finland. https://doi.org/ISBN 978–952–244–678–7

Veikkolainen, T., Kukkonen, I.T., 2019. Highly varying radiogenic heat production in Finland, Fennoscandian Shield. Tectonophysics 750, 93–116. https://doi.org/10.1016/j.tecto.2018.11.006

Wang, Z., Wang, F., Liu, J., Ma, Z., Han, E., Song, M., 2017. Field test and numerical investigation on the heat transfer characteristics and optimal design of the heat exchangers of a deep borehole ground source heat pump system. Energy Convers. Manag. 153, 603–615. https://doi.org/10.1016/j.enconman.2017.10.038

Welsch, B., 2019. Technical, Environmental and Economic Assessment of Medium Deep Borehole Thermal Energy Storage Systems, Technische, ökonomische und ökologische Bewertung mitteltiefer Erdwärmesondenspeicher. Technische Universität Darmstadt.

Zhou, C., Zhu, G., Xu, Y., Yu, J., Zhang, X., Sheng, H., 2015. Novel methods by using non-vacuum insulated tubing to extend the lifetime of the tubing. Front. Energy 9, 142–147. https://doi.org/10.1007/s11708-015-0357-7